Bioorganic & Medicinal Chemistry Letters 19 (2009) 6353–6357

Contents lists available at ScienceDirect

Bioorganic & Medicinal Chemistry Letters

journal homepage: www.elsevier.com/locate/bmcl

Design of novel α7-subtype-preferring nicotinic acetylcholine receptor agonists: Application of docking and MM-PBSA computational approaches, synthetic and pharmacological studies

Giovanni Grazioso [a,*], Diego Yuri Pomè [a], Carlo Matera [a], Fabio Frigerio [a], Luca Pucci [b], Cecilia Gotti [b], Clelia Dallanoce [a], Marco De Amici [a]

[a] Dipartimento di Scienze Farmaceutiche 'Pietro Pratesi', Università degli Studi di Milano, Via Mangiagalli 25, 20133 Milano, Italy
[b] CNR, Istituto di Neuroscienze, Farmacologia Cellulare e Molecolare e Dipartimento di Farmacologia, Chemioterapia e Tossicologia Medica, Università degli Studi di Milano, Via Vanvitelli 32, 20129 Milano, Italy

ARTICLE INFO

Article history:
Received 30 July 2009
Revised 11 September 2009
Accepted 18 September 2009
Available online 24 September 2009

Keywords:
MM-PBSA
Neuronal nicotinic acetylcholine receptors
α7 Selective nicotinic agonists
Binding affinity

ABSTRACT

In the search for nicotinic acetylcholine receptor (nAChRs) agonists with a selective affinity for the homomeric α7 channels, we carried out the virtual screening of a test set of potential nicotinic ligands, and adopted a simplified MM-PBSA approach to estimate their relative binding free energy values. By means of this procedure, previously validated by a training set of compounds, we reached a realistic compromise between computational accuracy and calculation rate, and singled out a small group of novel structurally related derivatives characterized by a promising theoretical affinity for the α7 subtype. Among them, five new compounds were synthesized and assayed in binding experiments at neuronal α7 as well as α4β2 nAChRs.

Neuronal nicotinic acetylcholine receptors (nAChRs), which are members of the four transmembrane domain superfamily of neurotransmitter-gated ion channels, are pentameric combinations of α and α/β subunits, with a high degree of complexity conferred by 12 different α (α2–α10) and β (β2–β4) subunits.[1,2] Hence, a large repertoire of molecular architectures can be generated, and the functional relevance of these subunit compositions has yet to be fully clarified.[1,2] Although neuronal nAChRs play an array of critical roles in the central nervous system (CNS), only in the last two decades a rapidly growing understanding of subtype localization has been associated with potential therapeutic applications. Indeed, the most abundant nAChR subtypes in the CNS are α4β2 heteromers and α7 homomers. The α4β2 subtypes are expressed predominantly in the cortex, hippocampus, visual cortex, striatum and substantia nigra, mesocorticolimbic pathway, and nucleus raphe magnus, whereas the α7 subtypes are mainly localized in the cortex, hippocampus, and auditory cortex.[3] Functionally, α7 channels are easily distinguished from α4β2-containing receptors due to their lower affinity for acetylcholine, a high affinity toward α-bungarotoxin, a rapid desensitization, and a relatively high permeability to calcium.[3,4] The improved knowledge of the role played by the two cited subtypes in cognitive processes (attention, memory), mood, nociception, and neuroprotection has encouraged the development of subtype-selective compounds designed for different pathologies of the CNS, including Alzheimer's and Parkinson's diseases, attention deficit hyperactivity disorder (ADHD), schizophrenia, epilepsy, Tourette's syndrome, anxiety, depression, and nicotine addiction.[5,6] Recently, the role of nAChRs has expanded from the modulation of specific neuroprotective mechanisms to central regulation of inflammatory properties, which predominantly involves the homopentameric α7 channel, thus disclosing an innovative therapeutic target for arthritis.[2] Worth mentioning, an alternative approach to the design and synthesis of compounds specifically targeting nAChR subtypes is the investigation of allosteric agents, mainly positive allosteric modulators, which is an emergent research theme especially with regard to α7 receptors.[7,8]

We recently investigated the binding mode of representative agonists of α7 nAChRs by performing molecular docking, cluster analysis, geometry optimizations and sampling with molecular dynamics (MD), and molecular mechanics Poisson–Boltzmann surface area (MM-PBSA) binding free energy calculations.[9] With this protocol, based on MD simulations of fully solvated protein–ligand complexes, we estimated the contribution of both polar and nonpolar terms as well as entropy to the overall free energy of binding. Since the calculated values were in good agreement with the experimental data, the MM-PBSA method emerged as a flexible theoretical tool for the rational design of ligands targeting the

* Corresponding author.
E-mail address: giovanni.grazioso@unimi.it (G. Grazioso).

0960-894X/$ - see front matter © 2009 Elsevier Ltd. All rights reserved.
doi:10.1016/j.bmcl.2009.09.073

neuronal α7 nAChR subtype. However, the robustness of the MM-PBSA approach was paid for in terms of computational time, since the procedure required a laborious calculation of the entropic factors.

In this study, we took into account on one hand the results reported by Borea et al.[10] which, through thermodynamic experiments, provided evidence that the binding of nicotinic agonists is mostly enthalpy driven. Moreover, we considered the approach described by Ferrari et al.,[11] which allowed correlation of the experimental binding free energy values with the sum of enthalpic and solvation contributions ($\Delta G'_{bind}$), leading to a remarkable reduction of the calculation time (8 h/cpd, 4 cpu). On these premises, adapting our MM-PBSA procedure to that reported by Ferrari et al., in this Letter we initially calculated the $\Delta G'_{bind}$ of a training set of known α7 nAChR ligands. Next, the same computational procedure was applied to a series of new potential α7 nAChR ligands, and finally we synthesized and tested in binding assays some of the derivatives characterized by the lowest predicted $\Delta G'_{bind}$ for the studied receptor subtype.

At first, we selected a group of 16 nAChR agonists reported in the literature and characterized by a relatively wide range of affinity for the α7 subtype; their molecular structures have been reproduced in Figure 1.

To this training set we applied the 3D model of the α7 nAChR previously reported by us,[9] which utilized as reference structure the crystallographic coordinates of *A*-AChBP co-crystallized with the full agonist (−)-epibatidine (PDB code 2BYQ). The ligands were docked at the MD-refined α7 nAChR binding pockets by means of the genetic-based algorithms docking program GOLD 3.1.[12] The active-site radius was set equal to 10 Å from the indole nitrogen of Trp147 responsible for the primary ligand anchoring point. Next, cluster analysis was carried out on the outputs of the docking program. To preliminarily assess the clusterability of docking outputs, a simple test (H* test) based on the work of Hopkins[13] was applied. Cluster analysis should be carried out only when $H^* \rightarrow 1$. If the H* test output was $0.6 < H^* < 1$, the hierarchical-agglomerative script (*AClAP*)[14] was applied to select a solution and, therefore, a statistically significant binding mode. The obtained α7 nAChR complexes were refined by means of a short molecular dynamics simulations (0.5 ns) applying our previously reported computational parameters.[9] Then, a minimization of the entire ensembles was performed setting a convergence criterion on the gradient of 0.05 kcal mol^{-1} $Å^{-1}$.

The evaluation of the $\Delta G'_{bind}$ was performed by means of the MM-PBSA approach on the minimized complexes (Eq. 1):

$$\Delta G'_{bind} = G'_{compl} - (G'_{rec} + G'_{lig}) \quad (1)$$

Each thermodynamic term contributing to the complex formation was computed by the *sander* and *mm-pbsa.pl* internal modules of the AMBER 9 package according to (Eq. 2):

$$G'_x = U_x^{gas} + W_x^{solv} \quad (2)$$

where U_x^{gas} is the term calculated by molecular mechanics (MM) methods and is the result of different contributions: $U_{bond} + U_{angle} + U_{torsion} + U_{vdW} + U_{ele}$. The terms U_{bond}, U_{angle}, and $U_{torsion}$ turn out to be zero when the single trajectory approach is applied, while the terms U_{vdW} and U_{ele} are the main parameters contributing to the $\Delta G'_{bind}$ value. W_x^{solv} is the solvation energy term and results from the sum of W_{polar} and $W_{nonpolar}$, where W_{polar} comes from the solution of the linear Poisson–Boltzmann equation and $W_{nonpolar}$ is the result of scaling the solvent accessible surface area by an appropriate surface tension.

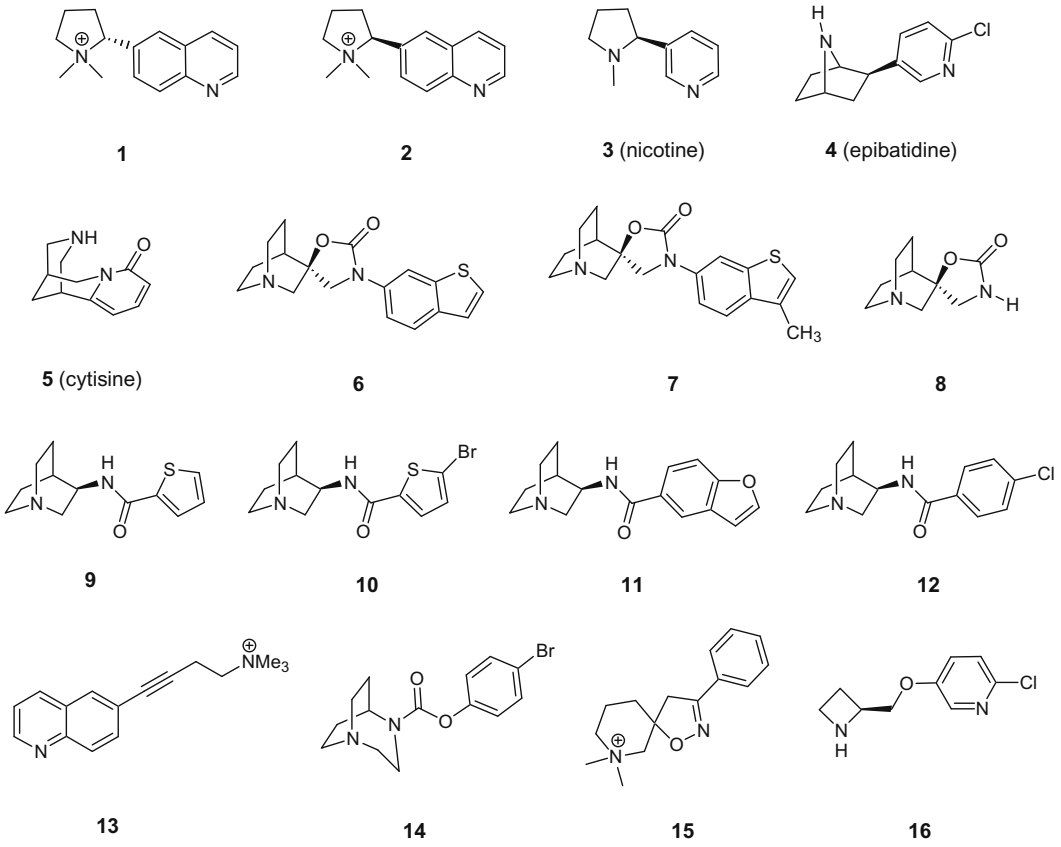

Figure 1. Chemical structures of the compounds inserted in the training set.

The data obtained on the training set confirmed the reliability of the applied computational protocol, particularly when the results were compared with those from other computationally faster methods in use for affinity prediction, such as the GOLD score and the pure enthalpic estimation (Table 1).

In fact, the calculated $\Delta G'_{bind}$ and the experimental binding free energy values showed better correlation and predictivity ($R^2 = 0.81$, leave-one-out cross-validated $q^2 = 0.75$) with the MM-PBSA procedure, since application of the GOLD score ($R^2 = 0.44$, $q^2 = 0.34$) and the enthalpic ($R^2 = 0.71$, $q^2 = 0.61$) protocols gave poorer results. Worth mentioning, for **3** (nicotine) and **8** we simulated a binding mode involving the presence of water molecules as hydrogen bond bridges, as it has been hypothesized in the literature for 'shorter' ligands.[15,16] Unfortunately, such a contribution cannot be estimated by the standard MM-PBSA algorithm, which results in underestimated theoretical $\Delta G'_{bind}$ values for **3** and **8**. Indeed, the correlation with MM-PBSA is improved ($R^2 = 0.86$, $q^2 = 0.83$) if the latter compounds are considered as outliers.

The validated computational method was then applied to predict the affinity of a test set of unknown compounds. The structure of nicotinic agonists may be exemplified by a formula in which a cationic head (protonatable or permanent) is linked to a substituted heteroaromatic ring with a hydrogen bond acceptor function.[17] About 150 compounds matching this general skeleton were considered in this study, combining the substructures reported in Figure 2. In this set of compounds, saturated (7-azabicyclo[2.2.1]heptane and 1-azabicyclo[2.2.2]octane) or unsaturated (7-azabicyclo[2.2.1]hept-2-ene and 1-azabicyclo[2.2.2]oct-2-ene) moieties bearing the charged nitrogen were connected with three heterocyclic rings (pyridine, quinoline, and isoquinoline) to which various R^2 substituents were appended in different positions. The choice of R^2 was based on (a) the synthetic feasibility of the investigated compounds, that is, the commercial availability of suitable building blocks, and (b) a degree of structural diversity combined with the improvement of the ligand molecular recognition by the α7 nAchR. To this end, for example, the bulky morpholine or piperazine rings were inserted as R^2 substituents in compounds characterized by pyridine as the aromatic fragment. In fact, the presence of a bulky group in this portion of the ligand molecular skeleton might be a requirement to gain selectivity for the α7 subtype, since this channel is slightly larger than the α4β2 channel, as it has been demonstrated by molecular dynamics simulations.[16]

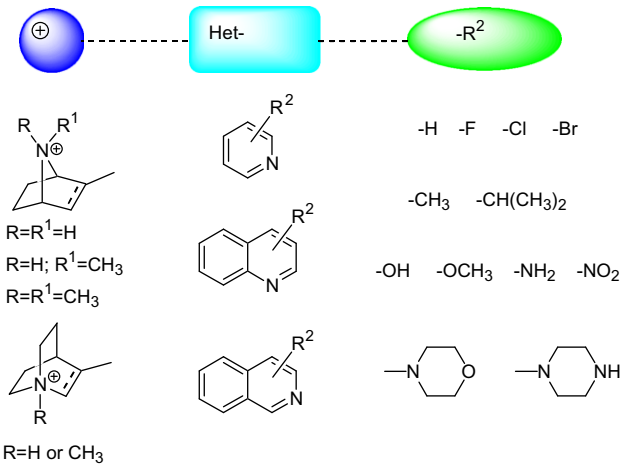

Figure 2. Structural fragments of potential nAChR ligands belonging to the test set.

Table 1
Binding free energy terms calculated for the training set of compounds

Compd	*G* score	ΔU_x^{gas} (kcal/mol)	$\Delta G'_{bind}$ (kcal/mol)	ΔG_{exp}
1	56.02	−253.02	−42.32	−9.67[a]
2	62.74	−248.86	−38.69	−7.96[a]
3	71.99	−242.78	−30.30	−7.06[b]
4	51.20	−264.47	−44.06	−10.70[b]
5	76.59	−256.80	−35.72	−7.38[c]
6	74.74	−270.39	−47.03	−10.36[d]
7	66.52	−275.08	−49.89	−11.69[d]
8	62.43	−253.16	−36.32	−9.65[e]
9	67.10	−266.08	−41.34	−9.74[f]
10	56.95	−270.62	−47.39	−11.52[f]
11	60.31	−271.21	−51.49	−12.07[g]
12	78.89	−268.65	−49.80	−10.41[c]
13	49.39	−260.64	−45.71	−9.40[a]
14	42.10	−268.40	−46.31	−10.77[h]
15	72.96	−251.38	−39.52	−8.44[i]
16	58.25	−259.16	−36.94	−7.64[l]

ΔU_x^{gas} terms resulted from the application of Eqs. 1 and 2 without the solvation contribution (W_x^{solv}).
The experimental binding free energy values were calculated on the basis of the K_i values reported by [a]Kottalam, J. et al. *Biopolymers* **1990**, *29*, 1409; [b]Jorgensen, W. L. et al. *J. Chem. Phys.* **1983**, *79*, 926; [c]Hall, M. et al. *Brain Res.* **1993**, *600*, 127; [d]Tatsumi, R. et al. *J. Med. Chem.* **2006**, *49*, 4374; [e]Mullen, G. et al. *J. Med. Chem.* **2000**, *43*, 4045; [f]Tatsumi, R. et al. *J. Med. Chem.* **2005**, *48*, 2678; [g]Wishka, D. G. et al. *J. Med. Chem.* **2006**, *49*, 4425; [h]Biton, B. et al. *Neuropsychopharmacology* **2007**, *32*, 1; [i]De Amici, M. et al., unpublished results; [l]Holladay, M. W. et al. *J. Med. Chem.* **1998**, *41*, 407.

The application of the above described computational protocol, based on the simplified version of the MM-PBSA approach, indicated that the lowest predicted $\Delta G'_{bind}$ values were invariably associated with compounds characterized by the mutual presence of the pyridine and morpholine moieties, such as derivatives **17–21** depicted in Figure 3. As a consequence, we planned to synthesize and test these structural analogues, together with 3-(pyridin-3-yl)-1-azabicylo[2.2.2]oct-2-ene **22** (Fig. 3), lacking the morpholine ring, which is a known ligand for neuronal nAChR subtypes.[18] We synthesized **22** according to the procedure described in the literature,[18] and used it as a reference compound in the binding affinity experiments after conversion into the corresponding fumarate.

The target derivatives **17–21** were obtained as racemates taking advantage of the carbon–carbon palladium-catalyzed Suzuki–Miyaura cross-coupling, a synthetic strategy richly documented in the recent literature.[19] Thus, as depicted in Scheme 1, the key step in the reaction sequences was the treatment of the known vinyl trifluoromethanesulfonates **23**[20] and **25**[21] with 6-(morpholin-4-yl)pyridine-3-boronic acid pinacol ester, using tetrakis(triphenylphosphine)palladium(0) as the catalyst and similar experimental conditions. The unsaturated *N*-Boc intermediate **24** (77% yield from triflate **23**) was reacted with a 4 N solution of HCl in dioxane, and the resulting hygroscopic hydrochloride of **17** was isolated after a few washings with anhydrous diethyl ether. Conversely, the desired 3-(6-morpholin-4-yl-pyridin-3-yl)-1-azabicyclo[2.2.2]oct-2-ene **18**, obtained in 74% yield from triflate **25**,[22] was transformed into the crystalline fumarate and iodomethylate **19**, respectively.[23] Furthermore, derivative **18** underwent a standard catalytic hydrogenation of the carbon–carbon double bond, which gave *endo*-**26** as the sole isomer in almost quantitative yield. Epimerization of **26** to the desired *exo*-3-(6-morpholin-4-yl-pyridin-3-yl)-1-azabicyclo[2.2.2]octane **20** proceeded in 91% yield, using potassium *tert*-butoxide in refluxing *tert*-butyl alcohol (Scheme 1).[24] Then, the quinuclidine derivative **20** afforded its corresponding fumarate and methyl iodide **21**. Since we planned to synthesize also the saturated *exo*-analogue of **17**, we submitted intermediate **24** to catalytic hydrogenation, which provided the expected *endo*-*N*-Boc isomer (not reported in Fig. 3). However, the above cited epimerization procedure failed when applied on the latter derivative or its corresponding free amine.

The target derivatives **17–21** and the reference compound **22** were assayed for binding affinity at rat α7 and α4β2 nAChRs, using [^{125}I]α-bungarotoxin and [^{3}H]epibatidine as radioligands, respec-

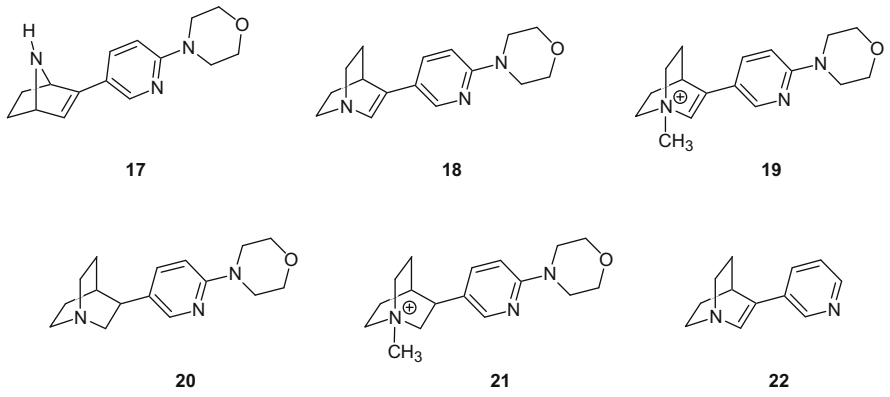

Figure 3. Compounds synthesized and tested in this study.

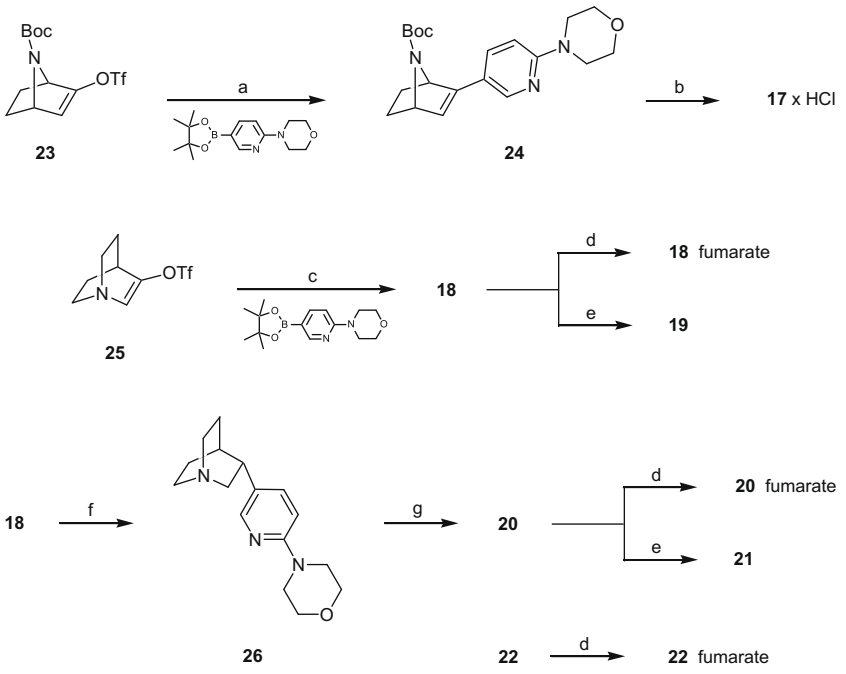

Scheme 1. Reagents and conditions: (a) $Pd(PPh_3)_4$, K_2CO_3, DME/H_2O (5:1), 80 °C; (b) 4 N HCl/dioxane, Et_2O; (c) $Pd(PPh_3)_4$, Na_2CO_3 (aq), THF, 80 °C; (d) $C_4H_4O_4$, MeOH; (e) CH_3I, MeOH; (f) H_2, 10% Pd/C; (g) *tert*-BuOK/*tert*-BuOH, reflux, 50 h.

tively, according to a previously described experimental protocol.[25] The K_i values, which were calculated from the competition curves of three separate experiments by means of the LIGAND program,[26] are gathered in Table 2 together with the corresponding predicted $\Delta G'_{bind}$ for the α7 subtype. In this respect, even though five compounds are not statistically significant, the correlation between the experimental and theoretical data was acceptable if derivatives 17–**21** are taken into account ($R^2 = 0.51$). In analogy with derivatives **3** and **8** belonging to the training set, the reference ligand **22** behaved as an outlier, since the molecular dynamics simula-

Table 2
MM-PBSA predicted relative binding free energy ($\Delta G'_{bind}$) values at α7 nAChRs for compounds **17**–**22**, and experimental affinity data (K_i) for the same derivatives at native α7 and α4β2 nAChRs present in rat cortical membranes

Compd	$\Delta G'_{bind}$ (kcal/mol)	α7 [^{125}I]α-Bungarotoxin K_i[a] (μM)	α4[^{3}H]-Epibatidine K_i[a] (μM)	Selectivity (α7:α4β2)
17	−42.75	33 (42)	12 (23)	0.4
18	−50.00	0.40 (27)	3.10 (25)	7.8
19	−47.45	5.60 (36)	22 (23)	3.9
20	−48.04	0.35 (27)	21 (17)	60
21	−50.34	6.10 (36)	25 (17)	4.1
22	−36.35	0.14[b] (32)	0.11[c] (15)	0.8

Numbers in brackets represent % coefficients of variation.
[a] The K_i values were all calculated using the LIGAND program (Ref. 26).
[b] K_i = 0.085 μM (Ref. 18), measured against [^{3}H]MLA as the radioligand, and calculated using the Cheng and Prusoff equation (Ref. 27).
[c] K_i = 0.0076 μM (Ref. 18), measured against the same radioligand and calculated using the Cheng and Prusoff equation (Ref. 27).

tions demonstrated that its binding affinity is mediated by a water molecule.

The overall pharmacological data show that the morpholine ring does not improve the affinity at the α7 nAChRs, since the most affinitive morpholine-containing ligands **18** and **20** (K_i = 0.40 and K_i = 0.35 μm, respectively) gave comparable results to that of their parent compound **22** (K_i = 0.14 μm), which lacks morpholine. However, the presence of morpholine, which lowers the affinity for the α4β2 receptors, positively affects the subtype selectivity, as evidenced by the value of α7 versus α4β2 ratio on passing from **22** (0.8) to **18** (7.8) (Table 2). This trend is markedly reinforced when the saturated quinuclidinyl derivative **20** is taken into account, whose α7 versus α4β2 ratio is equal to 60. On the other hand, the two quaternary ammonium analogues **19** and **21** display a lower α7 affinity, and, consequently, a negligible degree of discrimination between the subtypes.

Indeed, visual inspection of the ligand–α7 nAChR complexes indicates that the morpholine ring of **18** and **20** can be located favorably in a sub-pocket defined by the three residues Gln116, Tyr117, and Ser149 of the α7 receptor, which correspond to β2-Phe117, β2-Trp118, and α4-Thr150 of the α4β2 subtype. The presence of the Gln-Tyr-Ser rather than the Phe-Trp-Thr sequence confers a more hydrophilic character to the α7 sub-site, which, coupled with the reduced size and the higher flexibility of the involved residues, allows to host sterically hindered substituents such as morpholine.

In summary, the structure-based design of α7-nAChR agonists may take advantage of a relatively expeditious computational protocol, which, by exploiting a previous model of the target receptor subtype, made use of GOLD for pose generation, AClAP for cluster analysis, and AMBER 9 for the MM-PBSA calculations. Thus, after validating the methodology, we predicted the affinity of a series of potential nicotinic ligands, selected a small set of structural analogues, and obtained two novel selective α7-nAChR agonists with a binding affinity in the low micromolar range.

Acknowledgments

This research has been financially supported by the Italian PRIN Grant # 20072BTSR2 (M.D.A. and C.G.). G.G. and D.Y.P. are indebted to the CILEA Consortium for the supercomputer time provided on the 'lagrange' cluster.

References and notes

1. Romanelli, M. N.; Gratteri, P.; Guandalini, L.; Martini, E.; Bonaccini, C.; Gualtieri, F. *ChemMedChem* **2007**, *2*, 746.
2. Lippiello, P. M.; Bencherif, M.; Hauser, T. A.; Jordan, K. G.; Letchworth, S. R.; Mazurov, A. A. *Exp. Opin. Drug Discovery* **2007**, *2*, 1185.
3. Gotti, C.; Zoli, M.; Clementi, F. *Trends Pharmacol. Sci.* **2006**, *27*, 482.
4. Dajas-Bailador, F.; Wonnacott, S. *Trends Pharmacol Sci.* **2004**, *25*, 317.
5. Gotti, C.; Clementi, F. *Prog. Neurobiol.* **2004**, *74*, 363.
6. Cincotta, S. L.; Yorek, M. S.; Moschak, T. M.; Lewis, S. R.; Rodefer, J. S. *Curr. Opin. Invest. Drugs* **2008**, *9*, 47.
7. Bertrand, D.; Gopalakrishnan, M. *Biochem. Pharmacol.* **2007**, *74*, 1155.
8. Faghih, F.; Gopalakrishnan, M.; Briggs, C. A. *J. Med. Chem.* **2008**, *51*, 701.
9. Grazioso, G.; Cavalli, A.; De Amici, M.; Recanatini, M.; De Micheli, C. *J. Comput. Chem.* **2008**, *29*, 2593.
10. Borea, P. A.; Varani, K.; Gessi, S.; Merighi, S.; Dal Piaz, A.; Gilli, P.; Gilli, G. *Curr. Top. Med. Chem.* **2004**, *4*, 361.
11. Ferrari, A. M.; Degliesposti, G.; Sgobba, M.; Rastelli, G. *Bioorg. Med. Chem.* **2007**, *15*, 7865.
12. Jones, G.; Willett, P.; Glen, R. C.; Leach, A. R.; Taylor, R. *J. Mol. Biol.* **1997**, *267*, 727.
13. Hopkins, B. *Ann. Bot. (Oxford, UK)* **1954**, *18*, 213.
14. (a) Bottegoni, G.; Cavalli, A.; Recanatini, M. *J. Chem. Inf. Model.* **2006**, *46*, 852; (b) Bottegoni, G.; Rocchia, W.; Recanatini, M.; Cavalli, A. *Bioinformatics* **2006**, *22*(14), e58.
15. Celie, P. H. N.; Van Rossum-Fikkert, S. E.; Van Dijk, W. J.; Brejc, K.; Smit, A. B.; Sixma, T. K. *Neuron* **2004**, *41*, 907.
16. Huang, X.; Zheng, F.; Chen, X.; Crooks, P. A.; Dwoskin, L. P.; Zhan, C. G. *J. Med. Chem.* **2006**, *49*, 7661.
17. Guandalini, L.; Martini, E.; Dei, S.; Manetti, D.; Scapecchi, S.; Teodori, E.; Romanelli, M. N.; Varani, K.; Greco, G.; Spadola, L.; Novellino, E. *Bioorg. Med. Chem.* **2005**, *13*, 799.
18. Seifert, S.; Gündisch, D.; Tilotta, M. C.; Seitz, G. *Pharmazie* **2003**, *58*, 353.
19. (a) Nicolaou, C.; Bulger, P. G.; Sarlah, D. *Angew. Chem., Int. Ed.* **2005**, *44*, 4442; (b) Yin, L.; Liebscher, J. *Chem. Rev.* **2007**, *107*, 133; (c) Doucet, H. *Eur. J. Org. Chem.* **2008**, *12*, 2013.
20. (a) Carroll, F. I.; Liang, F.; Navarro, H. A.; Brieaddy, L. E.; Abraham, P.; Damaj, M. I.; Martin, B. R. *J. Med. Chem.* **2001**, *44*, 2229; (b) Rizzi, L.; Dallanoce, C.; Matera, C.; Magrone, P.; Pucci, L.; Gotti, C.; Clementi, F.; De Amici, M. *Bioorg. Med. Chem. Lett.* **2008**, *18*, 4651.
21. Gohlke, H.; Gündisch, D.; Schwarz, S.; Seitz, G.; Tilotta, M. C.; Wegge, T. *J. Med. Chem.* **2002**, *45*, 1064.
22. *3-(6-Morpholin-4-yl-pyridin-3-yl)-1-azabiciclo[2.2.2]oct-2-ene* (**18**): A solution of enoltriflate **25** (318 mg, 1.24 mmol) in THF (6 mL) was dropped into a magnetically stirred mixture of 6-(morpholin-4-yl)pyridine-3-boronic acid pinacol ester (450 mg, 1.55 mmol) in THF (6 mL), 2 M aqueous Na_2CO_3 (2.5 mL), and $Pd(PPh_3)_4$ (30 mg, 0.025 mmol). After heating at 80 °C under stirring for 20 h, water (30 mL) was added and the reaction mixture was extracted with dichloromethane (4 × 40 mL). The combined organic extracts were dried over sodium sulfate, and, after concentration under reduced pressure, the residue was purified by silica gel column chromatography ($CH_2Cl_2 \rightarrow CH_2Cl_2$/MeOH 9:1) to afford 248 mg (74% yield) of the desired derivative **18** as a pale yellow oil. R_f = 0.45 (25% methanol/dichloromethane). ^{1}H NMR (300 MHz, $CDCl_3$): δ 1.57 (m, 2H), 1.77 (m, 2H), 2.68 (m, 2H), 3.05 (m, 3H), 3.47 (m, 4H), 3.75 (m, 4H), 6.58 (d, *J* = 8.8 Hz, 1H), 6.69 (s, 1H), 7.51 (dd, *J* = 8.8 and 2.5 Hz, 1H), 8.21 (d, *J* = 2.5 Hz, 1H). ^{13}C NMR (75 MHz, $CDCl_3$): δ 27.42, 28.90, 45.75, 49.48, 66.86, 106.91, 121.74, 132.37, 134.33, 144.18, 144.63, 159.21. Anal. Calcd for $C_{16}H_{21}N_3O$ (271.36): C, 70.82, H, 7.80, N, 15.49. Found: C, 70.43; H, 7.61; N, 15.72.
23. *3-(6-Morpholin-4-yl-pyridin-3-yl)-1-azabiciclo[2.2.2]oct-2-ene* **18** × $C_4H_4O_4$: Colorless prisms (from 2-propanol), mp 205–207 °C, dec. ^{1}H NMR (300 MHz, CD_3OD): δ 1.82 (m, 2H), 2.15 (m, 2H), 3.15 (m, 2H), 3.31 (m, 1H), 3.56 (m, 4H), 3.62 (m, 2H), 3.77 (m, 4H), 6.71 (s, 2H), 6.85 (d, *J* = 9.1 Hz, 1H), 6.94 (s, 1H), 7.78 (dd, *J* = 9.1 and 2.5 Hz, 1H), 8.33 (d, *J* = 2.5 Hz, 1H). ^{13}C NMR (75 MHz, CD_3OD): δ 23.18, 28.09, 45.34, 50.21, 66.50, 107.14, 118.44, 120.71, 134.91, 135.02, 145.11, 145.18, 159.98, 169.74. Anal. Calcd for $C_{20}H_{25}N_3O_5$ (387.43): C, 62.00; H, 6.50; N, 10.85. Found: C, 61.88; H, 6.63; N, 10.94.
3-(6-Morpholin-4-yl-pyridin-3-yl)-1-azabiciclo[2.2.2]oct-2-ene methyl iodide **19**: Yellow-orange prisms (from 2-propanol), mp 210–215 °C, dec. ^{1}H NMR (300 MHz, CD_3OD): δ 1.94 (m, 2H), 2.25 (m, 2H), 3.33 (m, 3H), 3.44 (s, 3H), 3.57 (m, 4H), 3.62 (m, 1H), 3.78 (m, 4H), 3.85 (m, 1H), 6.88 (d, *J* = 9.1 Hz, 1H), 6.92 (s, 1H), 7.81 (dd, *J* = 9.1 and 2.5 Hz, 1H), 8.36 (d, *J* = 2.5 Hz, 1H). ^{13}C NMR (75 MHz, CD_3OD): δ 28.17, 28.29, 45.30, 50.09, 50.15, 50.21, 61.55, 66.50, 107.13, 117.66, 126.84, 126.90, 126.96, 135.24, 145.17, 145.43, 160.09. Anal. Calcd for $C_{17}H_{24}IN_3O$ (413.30): C, 49.40; H, 5.85; N, 10.17. Found: C, 49.73; H, 5.72; N, 9.87.
24. (a) Fletcher, S. R.; Baker, R.; Chambers, M. S.; Herbert, R. H.; Hobbs, S. C.; Thomas, S. R.; Verrier, H. M.; Watt, A. P.; Ball, G. R. *J. Org. Chem.* **1994**, *59*, 1771; (b) Zhang, C.; Trudell, M. L. *J. Org. Chem.* **1996**, *61*, 7189.
25. Dallanoce, C.; Bazza, P.; Grazioso, G.; De Amici, M.; Gotti, C.; Riganti, L.; Clementi, F.; De Micheli, C. *Eur. J. Org. Chem.* **2006**, 3746.
26. Munson, P. J.; Rodbard, D. *Ann. Biochem.* **1980**, *107*, 220.
27. Cheng, Y. C.; Prusoff, W. H. *Biochem. Pharmacol.* **1973**, *22*, 3099.